Grain boundary energies as a function of GB parameters

Vishal Subbiah, Vijay Bharadwaj J, Anand K Kanjarla

Department of Metallurgical and Materials Engineering, Indian Institute of Technology Madras, Chennai 600036, INDIA

Abstract

Grain boundary energy is an important factor to understand the nature of grain boundaries and its impact on material properties. Thus, it warrants for experimental and computational research to quantify grain boundary energy (GBE). In this work, we have used molecular dynamics simulation via LAMMPS to calculate GB energy of few FCC and BCC metals. We have observed that there is linear correlation between GB energy of elements with similar crystal structures. The size of system under consideration is observed not to have any considerable effect on the GB energy.

Keywords: Grain Boundary Engineering, Molecular Dynamics Simulation, Grain Boundary Energy, LAMMPS, Quaternions

1. Introduction

Crystalline materials exhibit long and short range order. By the virtue of solidification and processing of metals and alloys, crystallites of differing orientations impinge upon one another. This results in a defect called grain boundary. Thus, a grain boundary is an interface between two or more grains. Over the years, many models have been proposed to explain the structure and properties of grain boundaries. The parameters usually studied with respect to the grain boundaries are the misorientation and the energy associated with it. Based on the misorientation angle, low angle grain boundaries(LAGB) with misorientation $< 15^o$ are explained using lattice distortion model and high angle grain boundaries(HAGB) with misorientation $> 15^o$ are explained using coincident site lattice theory.

Lattice distortion model explains grain boundary as the interface between two grains of which one is tilted or twisted with respect to another. Based on the relative orientation between the rotation axis and the grain boundary plane, LAGB comes in tilt and twist varieties. When rotation axis is perpendicular to boundary plane, twist boundaries are observed as contrast to tilt boundaries which

Email addresses: subbiahvishal@gmail.com (Vishal Subbiah), jvijay1992@gmail.com (Vijay Bharadwaj J), kanjarla@iitm.ac.in (Anand K Kanjarla)

URL: https://mme.iitm.ac.in/kanjarla/ (Anand K Kanjarla)

are observed when rotation axis is parallel to boundary plane. If the neighbouring grains satisfy mirror symmetry, symmetrical tilt boundary is observed.

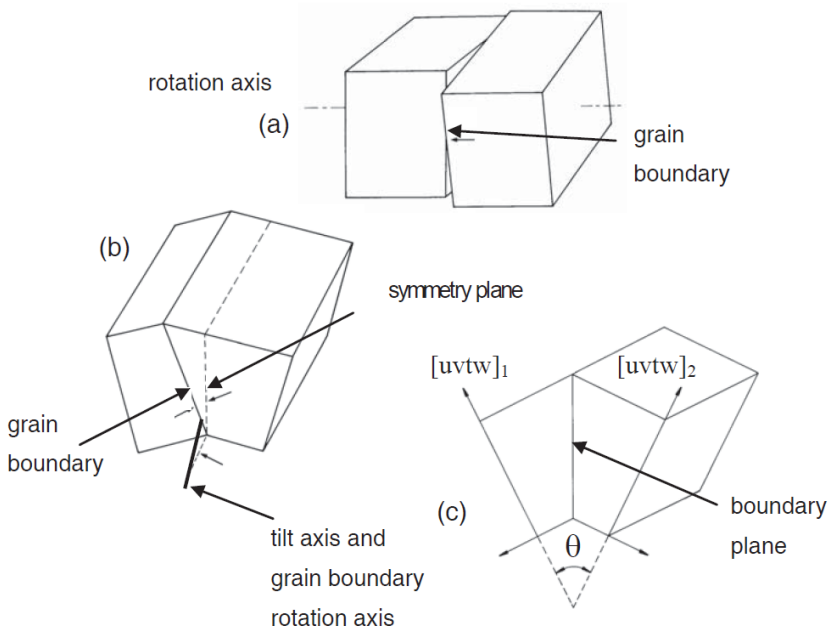

Figure 1: Schematic depictions of a) Twist grain boundary and b) Asymmetrical tilt and c) Symmetrical tilt boundary

However, when the misorientation is $> 15^{\circ}$, the lattice distortion model will no longer suffice to explain the observed properties [1]. When the adjacent grains satisfy certain misorientation conditions, certain fraction of the lattice points of the interpenetrated crystallites overlap forming a superlattice. This implies certain crystallographic planes transcend the grain boundary from one grain to another [2]. The overlapping lattice points are called coincidence sites and the superlattice is termed as coincident site lattice(CSL). This CSL is characterized by quantity Σ which is the reciprocal density of coinciding sites.

$$\Sigma = \frac{\text{volume of elementary cell CSL}}{\text{volume of elemetary cell of crystal lattice}} \tag{1}$$

Special boundaries have high density of coincident sites and have a low odd value for Σ. Experimental data shows that CSL boundaries with low Σ have low energy configuration which can be deduced from the low values for free surface energy and migration activation enthalpy. These special boundaries consist of one of the following polyhedral which are termed as structural units. When the misorientation is not of the required value, other structural units are introduced into the grain boundary whose density will increase or decrease with the misorientation angle. Eventually, the grain boundary will be comprise only of the new structural unit.

These special grain boundaries are of interest in engineering applications as they impart beneficial properties like resistance to intergranular degradation, grain boundary sensitization, dynamic embrittlement, solute segregation and Coble creep. Thus, characterization of these will aid in developing materials with better properties. In the process of characterization, understanding the structure and energy configuration of the boundary is very essential. Simulation is a very effective tool in understanding the energy of the grain boundary. Atomistic simulation and molecular dynamics simulation has been carried out in the literature [3] [4].

Their results shed light on effect of relaxation on GB energy and strong linear correlation between GB energy of various elements. Solute segregation is related to the grain boundary energy in binary alloys [5] through phase field crystal method (continuum method). The grain boundary energy versus the misorientation data is matched by the Read - Shockley theory. Grain boundary energy versus average alloy concentration are characterized by this theory. Simulation of grain boundaries at elevated temperatures to explain the GB migration mechanisms is present in literature [6]. Grain boundary study and grain boundary engineering are heavily dependent on visual representation for the analysis of boundary statistics and their connectivity. Some work has been done to improve the graphical representation of grain misorientation statistics and colourized maps of grain boundary misorientation [7].

In order to completely characterize a grain boundary, five independent parameters are necessary. The misorientation between adjacent grains can be quantified by the three Euler angles which are operated on grain A to generate grain B. The grain boundary plane is positioned using two more parameters in the form of miller indices {hkl}.The aim of this work is to use Molecular Dynamics (MD) simulations with LAMMPS [8] to investigate GB energy configuration as a function of misorientation angle in Al, Cu, Ni, Fe and Na [9] [10] [11] [12]. We have chosen an axis and have defined grain A. Using quaternions [13], grain B has been generated for varying misorientation angle ranging from 0˚to 90˚.

2. Molecular Dynamics Simulation of Grain Boundaries

We utilized the LAMMPS package to calculate the grain boundary energy based on the misorientation angle [14]. To calculate the energy for all the angles from 0^o to 90^o as seen in Fig. 3a. To do these calculations in the most optimal way, we wrote a script in python to automate this process as well as extract the relevant data i.e. the grain boundary energy from the log files generated for their respective misorientation angles.

It is well known that grain boundaries are based on five parameters. In our script we have defined the parameters through quaternions instead of orientation matrices as the time and space

Element	Al	Cu	Ni	Fe	Na
Structure	FCC	FCC	FCC	BCC	BCC
E_{coh} (eV)	-3.36	-3.54	-4.45	-4.12	-1.11

Table 1: Energy of perfect crystal per atom for different elements

complexity is significantly lesser, especially as the number of grain boundaries increases. Quaternions are represented by four terms instead of the nine terms required for the matrix orientation. To utilize the properties of quaternions we wrote a script to implement the operations required.

Currently the script is designed such that the researcher can calculate the grain boundary energy for a given misorientation angle for a given angle axis pair and a given reference grain. The researcher must also specify the cohesive energy for a given element. It can be expanded to include calculations for multiple temperatures, axis angle pairs, various reference orientations and elements. The mathematical equations utilized can be found in Appendix A.

Once the required orientations are calculated, it generates the LAMMPS input file and calls the LAMMPS package to calculate the grain boundary energy. It can be set to run in parallel or serial based on the researcher's requirement. The script also accounts for equilibration based on the temperature chosen, but the researcher needs to choose the number of iterations.

3. Calculation of the Grain Boundary Energy

In this work we calculate the grain boundary energy per unit area (mJ/m^2) [15]. The calculations required to find the energy are :

$$E_{gb} = \frac{(E_{Tot} - nE_{coh})}{A} \tag{2}$$

In the above equation, E_{gb} is the grain boundary energy per unit area. While E_{Tot} is the energy of the system and E_{coh} is the energy of a perfect crystal per atom. A is the area of the grain boundary while n is the number of atoms in the system.

To calculate the E_{coh}, we utilized LAMMPS to find the energy. The values obtained are seen in Table 1.

4. Results

The structure of the simulated grain boundaries was analysed using Ovito [16]. During the relaxations, it was observed that the atoms of adjacent grains close to the grain boundary slightly

dislodge from their lattice site and move to reduce the empty volume of the grain boundary. Since the empty volume of grain boundary is an essential factor in the calculation of GB energy, the movement of atoms near the grain boundaries is exhibited to lower the excess volume. The images of grain boundaries before and after relaxation are shown in Fig. 2a and Fig. 2b confirms this observation.

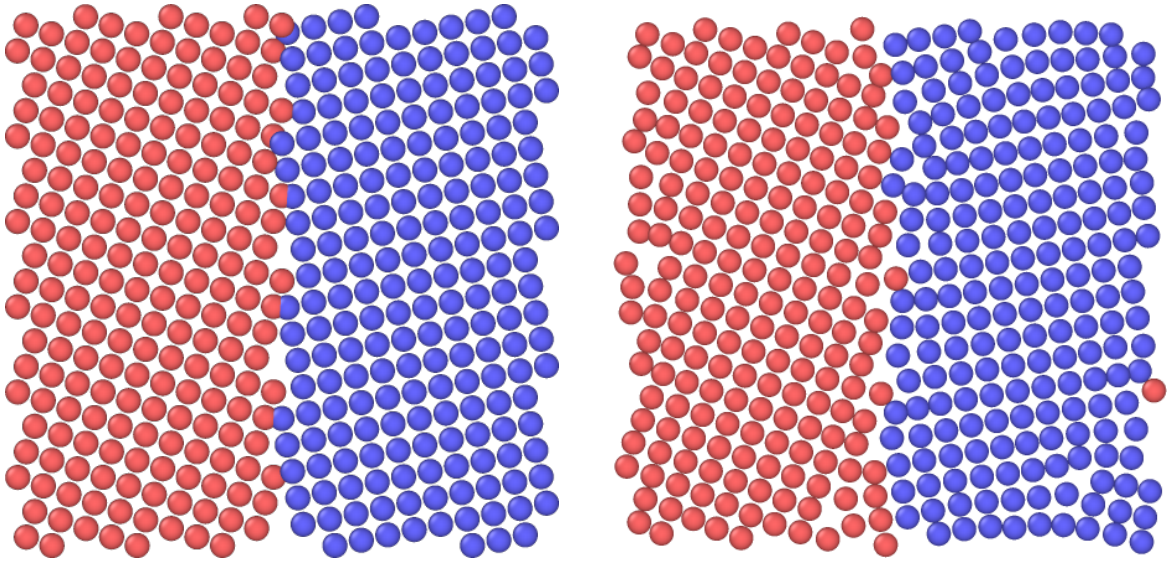

(a) Before (b) After

Figure 2: Schematic of Grain boundary before and after equilibration

The GB energies were calculated by choosing the axis as [100]. Since this axis has four fold symmetry, the misorientation angle was varied from 0^o to 90^o. The GB energies as a function of increasing misorientation are plotted in Fig. 3a. GB energies for the chosen special grain boundaries are depicted in 3b.

The GB energy shows smooth increase with misorientation in till 15^o in agreement with the literature [17]. For all misorientations, it can be observed that the GB energy of Ni followed by Cu and Al among the FCC metals. Fe has higher GB energy as compared to Na. This observation is valid for the GB energies of special grain boundaries also. When compared 1, it can be concluded that the element with higher cohesive energy has grain boundaries of higher energy. From Fig. 3c and Fig. 3d, it can be observed that Ni - Al line has a greater slope than Cu - Al line while the slope of Fe - Al line is greater than the slope of Na - Al line.

The graph depicting the GB energies of Al for system of 4000 and 32000 atoms as shown in Fig.

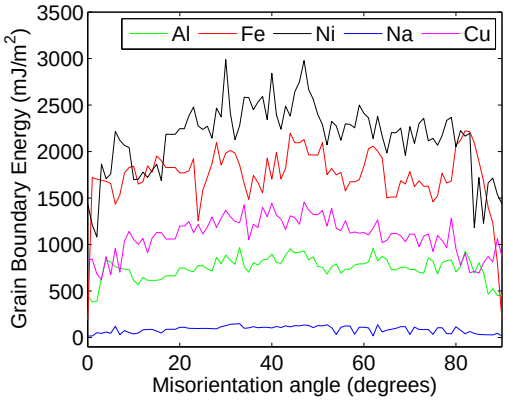

(a) Grain Boundary Energy for different elements at different misorientation angles for [100]

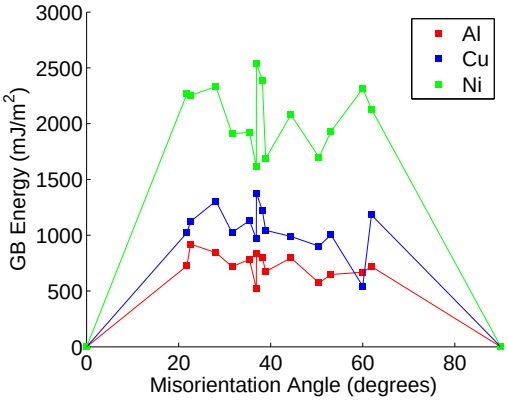

(b) Grain Boundary Energy for different elements at specific misorientation angles

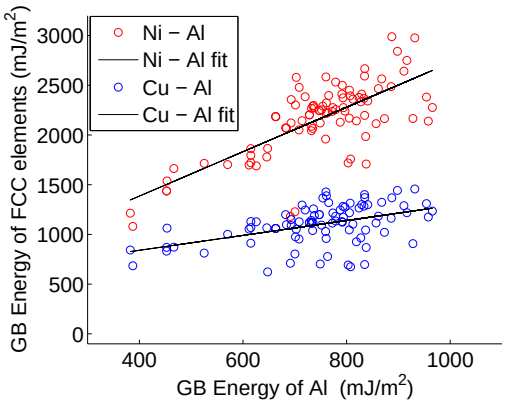

(c) The grain boundary energy of FCC elements with respect to the grain boundary energy of Al for [100]

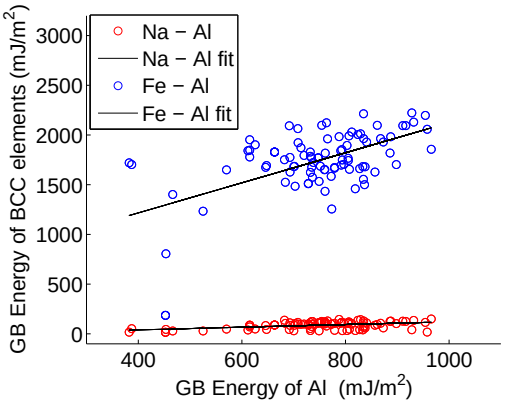

(d) The grain boundary energy of BCC elements with respect to the grain boundary energy of Al for [100]

Figure 3: Grain Boundary Energy Plots [18]

4a. To compare the relative energies, GB energy of system of 32000 atoms is plotted against the system of 4000 atoms 4b. In the surface plots 4c 4d, GB energy is plotted against misorientation angle for the systems of 4000 and 32000 atoms.

5. Discussion

GB energy calculation takes into account the energy of broken atomic bonds. Thus, GB energy is directly dependent on the cohesive energy. Consequently, the element with higher cohesive energy will have higher GB energy. This argument is supported by the results from the simulations. This discussion can be extended to explain the higher slope of Ni-Al line.

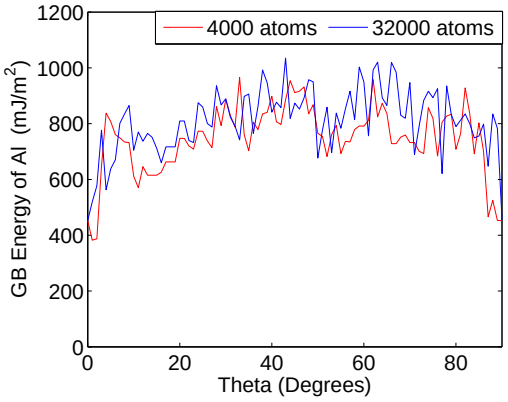

(a) Grain boundary energy for Al for two different number of atoms

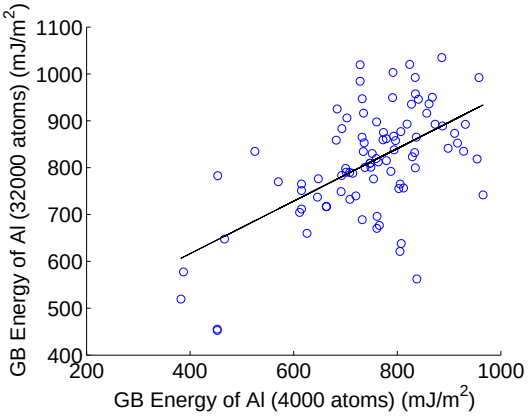

(b) Grain boundary energy for 32000 atoms with respect to its energy for 4000 atoms

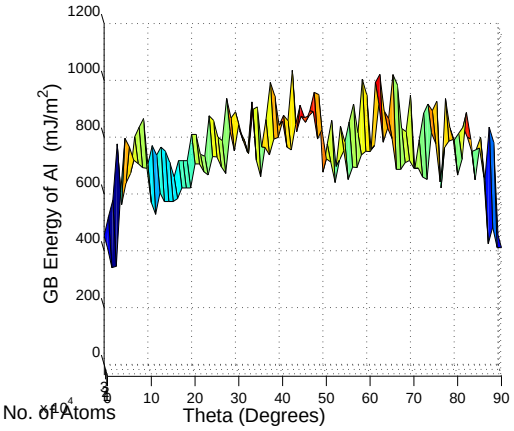

(c) Range of the grain boundary energy based on number of atoms

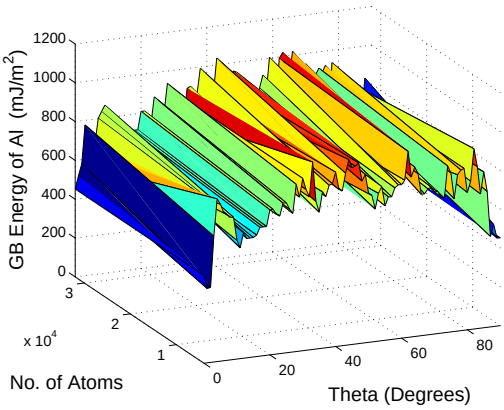

(d) 3D plot of grain boundary energy for Al

Figure 4: Grain Boundary Energy Plots based on number of atoms

There is a linear correlation between GB energies of various elements when normalized with a common element. This suggests that the grain boundaries are made up of similar structural units. This argument holds true for BCC metals also.

From the plots 4a 4b, we can conclude that by increasing the size of the system, there is no increase in GB energy. From the surface plots, we can estimate that the energy of a system having size with the bracket [4000,32000] will have the GB energy lying within the coloured region of Fig. 4c and Fig. 4d.

As mentioned, the code developed during this work can be used to calculate GB energies at higher temperatures also. We are expecting results for the GB energy of Al at 300 K.

Special Boundary	Axis/Angle	Al (mJ/m^2)	Ni (mJ/m^2)	Cu (mJ/m^2)
$\Sigma 3$	$([111], 60^o)$	668.3629477	2313.503264	542.6287626
$\Sigma 5$	$([100], 36.87^o)$	522.9487375	1611.694997	967.3479711
$\Sigma 5$	$([310], 36.9^o)$	838.3107299	2541.175746	1377.902998
$\Sigma 5$	$([210], 53.1^o)$	648.4360329	1930.204725	1003.61505
$\Sigma 7$	$([111], 38.2^o)$	799.59023991	2383.289551	1220.259885
$\Sigma 9$	$([110], 38.9^o)$	674.5446162	1686.042331	1043.711861
$\Sigma 11$	$([110], 50.5^o)$	572.6928924	1698.100215	902.1833643
$\Sigma 13$	$([510], 22.6^o)$	920.3526806	2253.155508	1123.398607
$\Sigma 13$	$([530], 61.9^o)$	719.7480073	2130.972587	1181.796138
$\Sigma 17$	$([410], 28.1^o)$	844.1934526	2331.234717	1306.500055
$\Sigma 21a$	$([111], 21.8^o)$	725.5228657	2266.003462	1022.717016
$\Sigma 21b$	$([211], 44.4^o)$	796.5469655	2079.544963	989.1332903
$\Sigma 27a$	$([110], 31.6^o)$	719.1078927	1910.453068	1024.067556
$\Sigma 27b$	$([210], 35.4^o)$	783.0839422	1921.599772	1130.470718

Table 2: Energies of special grain boundaries as seen in Fig. 3b

6. Conclusion

In this work, we have calculated the GB energy as a function of the misorientation angle, temperature, size of system for aluminium, copper, nickel, iron and sodium. We have observed that, as the cohesive energy of the system increases, the GB energy also increases. In this regard, Nickel has the highest GB energy among the considered FCC systems and Iron has highest among the considered BCC systems. Increasing the system size does not vary the GB energy considerably.

7. Acknowledgements

We would like thank Aditya Lakshmanan for his contribution towards this project. We would like to thank Dr. G. Phanikumar for the facilities of his group. We would like to thank IIT Madras for providing us access to their computational facilities. We thank the Metallurgical and Materials Engineering Department for giving us this opportunity to pursue this work.

References

[1] V. Randle, O. Engler, Introduction to Texture Analysis: Macrotexture, Microtexture and Orientation Mapping, CRC Press, 2014.
URL https://books.google.co.in/books?id=yJe9BwAAQBAJ

[2] X. Q. G. Gdui, L. Q. Nhlqhu, R. U. P. Yhuylhoilowljw, Z. Qrfk, U. Z. Zhughq, Fundamentals of grain boundaries and grain boundary migration.

[3] T. Uehara, N. Wakabayashi, Y. Hirabayashi, N. Ohno, An atomistic study of grain boundary stability and crystal rearrangement using molecular dynamics techniques, International Journal of Mechanical Sciences 50 (5) (2008) 956–965. doi:http://dx.doi.org/10.1016/j.ijmecsci.2007.09.001.
URL http://www.sciencedirect.com/science/article/pii/S0020740307001373

[4] E. A. Holm, D. L. Olmsted, S. M. Foiles, Comparing grain boundary energies in face-centered cubic metals: Al, Au, Cu and Ni, Scripta Materialia 63 (9) (2010) 905–908. doi:http://dx.doi.org/10.1016/j.scriptamat.2010.06.040.
URL http://www.sciencedirect.com/science/article/pii/S1359646210004331

[5] J. Stolle, N. Provatas, Characterizing solute segregation and grain boundary energy in binary alloy phase field crystal models, Computational Materials Science 81 (2014) 493–502. arXiv:1101.3464, doi:10.1016/j.commatsci.2013.09.002.
URL http://dx.doi.org/10.1016/j.commatsci.2013.09.002

[6] J.-E. Brandenburg, L. A. Barrales-Mora, D. A. Molodov, G. Gottstein, Effect of inclination dependence of grain boundary energy on the mobility of tilt and non-tilt low-angle grain boundaries, Scripta Materialia 68 (12) (2013) 980–983. doi:http://dx.doi.org/10.1016/j.scriptamat.2013.02.054.
URL http://www.sciencedirect.com/science/article/pii/S1359646213001425

[7] S. Patala, J. K. Mason, C. a. Schuh, Improved representations of misorientation information for grain boundary science and engineering, Progress in Materials Science 57 (8) (2012) 1383–1425. doi:10.1016/j.pmatsci.2012.04.002.
URL http://dx.doi.org/10.1016/j.pmatsci.2012.04.002

[8] S. Plimpton, Fast parallel algorithms for short range molecular dynamics, Journal of Computational Physics 117 (June 1994) (1995) 1–19. doi:10.1006/jcph.1995.1039.

[9] Y. Mishin, D. Farkas, M. Mehl, D. Papaconstantopoulos, Interatomic potentials for monoatomic metals from experimental data and ab initio calculations, Physical Review B 59 (5) (1999) 3393–3407. doi:10.1103/PhysRevB.59.3393.

[10] Y. Mishin, M. J. Mehl, D. A. Papaconstantopoulos, A. F. Voter, J. D. Kress, Structural stability and lattice defects in copper: \textit{Ab initio} , tight-binding, and embedded-atom calculations, Phys. Rev. B 63 (22) (2001) 224106. doi:10.1103/PhysRevB.63.224106.
URL http://link.aps.org/doi/10.1103/PhysRevB.63.224106

[11] M. I. Mendelev, S. Han, D. J. Srolovitz, G. J. Ackland, D. Y. Sun, M. Asta, Development of new interatomic potentials appropriate for crystalline and liquid iron, Philosophical Magazine 83 (35) (2003) 3977–3994. doi:10.1080/14786430310001613264.
URL http://www.tandfonline.com/doi/abs/10.1080/14786430310001613264

[12] S. R. Wilson, K. G. S. H. Gunawardana, M. I. Mendelev, Solid-liquid interface free energies of pure bcc metals and B2 phases, The Journal of Chemical Physics 142 (13) (2015) –. doi:http://dx.doi.org/10.1063/1.4916741.
URL http://scitation.aip.org/content/aip/journal/jcp/142/13/10.1063/1.4916741

[13] Euclideanspace - mathematics and computing.
URL http://www.euclideanspace.com

[14] M. A. Tschopp, D. L. Mcdowell, Asymmetric tilt grain boundary structure and energy in copper and aluminium, Philosophical Magazine 87 (25) (2007) 3871–3892. arXiv:http://dx.doi.org/10.1080/14786430701455321, doi:10.1080/14786430701455321.
URL http://dx.doi.org/10.1080/14786430701455321

[15] R. Alizadeh, Simulating Grain Boundary Energy Using Molecular Dynamics (May) (2014) 627–632.

[16] A. Stukowski, Visualization and analysis of atomistic simulation data with OVITOthe Open Visualization Tool, Modelling and Simulation in Materials Science and Engineering 18 (1) (2010) 15012.
URL http://stacks.iop.org/0965-0393/18/i=1/a=015012

[17] Y. L. B. Lin, X.M. Zhang, Acta Physica Sinica (1998) 583–588.

[18] MATLAB, version 7.10.0 (R2010a), The MathWorks Inc., Natick, Massachusetts, 2010.

Appendix A

Quaternion Representation:.

$$q = [q_w, q_x, q_y, q_z] \tag{3}$$

Where q_w, q_x, q_y and q_z are real numbers and q_x, q_y and q_z are along the 3 reference directions

Matrix Representation:.

$$M = \begin{bmatrix} m_{11} & m_{12} & m_{13} \\ m_{21} & m_{22} & m_{23} \\ m_{31} & m_{32} & m_{33} \end{bmatrix} \tag{4}$$

Each row in the above matrix represents the orientation along the direction of the reference orientation.

Axis/Angle Representation:.

$$< hkl > \theta^o \tag{5}$$

Here $< hkl >$ is the common crystal axis and θ^o is the rotation angle.

Axis/ Angle to Quaternions:.

$$q_w = cos(\theta/2) \tag{6}$$

$$q_x = hsin(\theta/2) \tag{7}$$

$$q_y = ksin(\theta/2) \tag{8}$$

$$q_z = lsin(\theta/2) \tag{9}$$

Quaternions to Matrix Orientation: .

$$M = \begin{bmatrix} 1 - 2q_y^2 - 2q_z^2 & 2q_xq_y - 2q_zq_w & 2q_xq_z + 2q_yq_w \\ 2q_xq_y + 2q_zq_w & 1 - 2q_x^2 - 2q_z^2 & 2q_zq_y - 2q_xq_w \\ 2q_xq_z - 2q_yq_w & 2q_yq_z + 2q_xq_w & 1 - 2q_y^2 - 2q_x^2 \end{bmatrix} \tag{10}$$